

# Pulsed Laser Deposition of Granular Co–Ag Thin Films

E. Agostinelli<sup>1\*</sup>, S. Alessandrini<sup>1</sup>, D. Fiorani<sup>1</sup>, A. Garcia Santiago<sup>1</sup>, A. M. Testa<sup>1</sup>, M. Angiolini<sup>2</sup> & M. Vittori-Antisari<sup>2</sup>

<sup>1</sup>ICMAT-CNR, Area della Ricerca di Roma, via Salaria km 29.500, PO Box 10, 00016 Monterotondo Scalo, Italy

<sup>2</sup>ENEA, INN-NUMA, CR Casaccia, CP 2400, 00100 Roma, Italy

**An investigation into the microstructural properties of  $\text{Co}_x\text{Ag}_{1-x}$  films, grown by pulsed laser deposition, as a function of deposition and post-deposition annealing temperature is reported. Surface morphology and microstructure were investigated by XPS, SEM and TEM measurements. Magnetic measurements were used to gain further information on particle size distributions through the analysis of the temperature dependence of the irreversible magnetization. Depending on cobalt content, deposition and post-deposition annealing temperature, the maximum of the cobalt grains diameter distribution was estimated to be in the range 2–6 nm. © 1998 John Wiley & Sons, Ltd.**

*Appl. Organometal. Chem.* **12**, 375–379 (1998)

**Keywords:** granular films; pulsed laser deposition; giant magnetoresistance; microstructure; magnetic properties

Received 12 December 1997; accepted 30

## INTRODUCTION

Granular metallic thin films have recently received a great deal of interest due to the occurrence of the so-called ‘giant magnetoresistance’ (GMR) effect. These materials consist of grains of a magnetic element (i.e. Fe, Co, Ni–Fe) distributed in a non-magnetic metallic matrix (i.e. Ag, Cu) where they are immiscible. The grain size and the intergrain distance are critical to obtaining a large GMR effect, since they have to be smaller than the spin-dependent mean free path (e.g. 5 nm within Co

particles and 27 nm in the Ag matrix<sup>1</sup>). However, there is a lower acceptable limit for the grain size, otherwise their magnetic moment becomes too small, as well as for the interparticle distance, which should not be too short since interparticle interactions reduce the GMR effect. This is the reason for the high sensitivity of GMR to deposition technique and deposition conditions.

Only a few examples of the preparation of such systems by the pulsed laser deposition (PLD) technique are known in the literature<sup>2–4</sup> and much work has still to be done in order to understand the correlation between microstructure and magnetic/transport properties.

In this framework, preliminary results are reported on the evolution of microstructural properties with deposition temperature and post-deposition annealing treatments in the system  $\text{Co}_x\text{Ag}_{1-x}$  ( $0.1 < x < 0.51$ ) deposited on Si(100). Surface morphology and microstructure investigations were performed by X-ray photoelectron spectroscopy (XPS), Scanning electron microscopy (SEM) and transmission electron microscopy (TEM) measurements. Moreover, magnetic measurements were used to gain further information on particle size distribution. In particular, through the analysis of the temperature dependence of the irreversible magnetization, the distribution of energy barriers for magnetization reversal of the single domain particles can be inferred.

## EXPERIMENTAL

Co–Ag thin films have been deposited by the PLD technique using an ArF excimer laser (wavelength 193 nm, pulse duration 17 ns FWHM, maximum repetition rate 50 Hz). Cold-pressed powders or metallic targets with defined stoichiometry ( $\text{Co}_x\text{Ag}_{1-x}$ ,  $0.1 < x < 0.5$ ) have been used to deposit on decapped or undecapped Si(100) sub-

\* Correspondence to: E. Agostinelli, ICMAT-CNR, Area della Ricerca di Roma, via Salaria km 29.500, PO Box 10, 00016 Monterotondo Scalo, Italy.  
E-mail: agostine@nserv.icmat.mlib.cnr.it

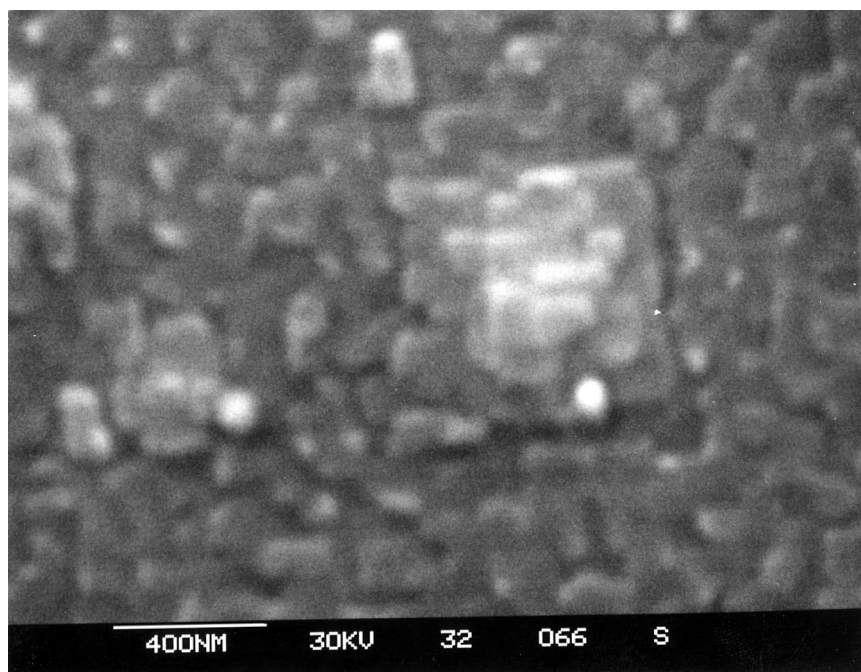


**Figure 1** SEM image of Co<sub>40</sub>Ag<sub>60</sub> granular film grown on etched Si(100), showing an oriented terrace growth mechanism.

strate. Film deposition was carried out in a stainless steel vacuum chamber ( $P = 1 \times 10^{-6}$  mbar maximum during film growth). In order to investigate the influence of different growth conditions on the microstructural and magnetic properties, different heat treatments have been carried out on samples with different Co concentrations: (1) deposition on heated substrate ( $50^\circ\text{C} < T_{\text{dep}} < 400^\circ\text{C}$ ); and (2) post-deposition annealing ( $200^\circ\text{C} < T_{\text{ann}} < 500^\circ\text{C}$ ). All the annealing procedures have been carried out in the deposition chamber at a pressure of  $1 \times 10^{-6}$  mbar and for a variable duration.

A Leica Cambridge S360 scanning electron microscope has been used for the analysis of film surface morphology. Specimens for TEM observations have been prepared in cross-sectional geometry and the final thinning was performed by Xe-ion beam milling on a stage cooled with liquid N<sub>2</sub>. TEM observations have been carried out with a JEOL 4000FX microscope equipped with analytical facilities and operated at 400 keV. The XPS spectra were obtained by means of a VG ESCA-LAB mk II instrument equipped with a hemispherical analyser operated in the constant analyser energy mode, with a pass energy of  $E_p = 20$  eV. The Al  $k_{1,2}$  ( $h = 1486.6$  eV) source was used to excite the photoemission, which was set at a constant

power of 300 W ( $15 \text{ kV} \times 20 \text{ mA}$ ). Ar<sup>+</sup> etching experiments on thin films were carried out using an ion gun in the analysis chamber. The atomic ratios were calculated from the area ratios of the corresponding components according to the procedure proposed by Wagner *et al.*<sup>5</sup> Measurements of magnetization versus temperature and hysteresis loops at 77 and 300 K were carried out by means of a commercial SQUID magnetometer (2–300 K;  $H_{\text{max}} = 55 \text{ kOe}$ ).

## RESULTS AND DISCUSSION

### Morphological, structural and chemical investigations

Film surfaces have been observed by SEM: within EDS (Energy Dispersive Spectroscopy) resolution for quantitative elemental analysis, all the samples showed, with only weak fluctuations, a homogeneous chemical composition close to the nominal one. As usual for films prepared by PLD, surfaces showed a number of molten droplets whose size ranged from 0.1 to 7  $\mu\text{m}$ ; the fraction of Co droplets was drastically reduced by increasing the laser

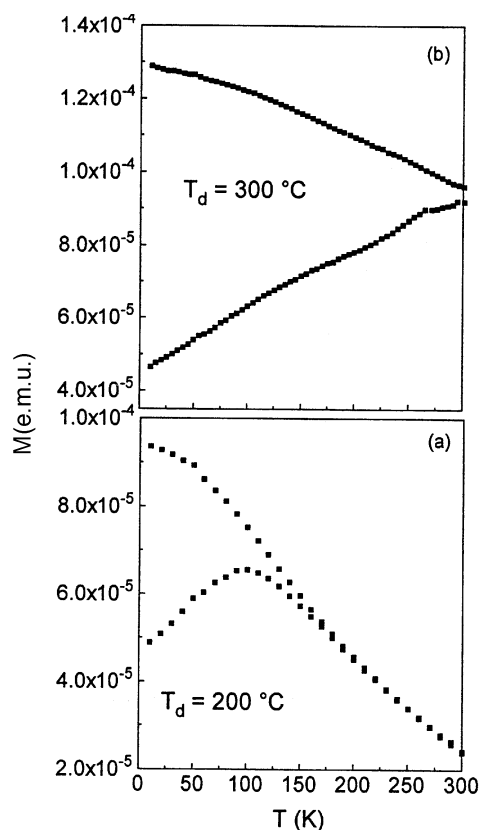


**Figure 2** FC and ZFC magnetization measurements as a function of temperature ( $H_a = 50$  Oe) for samples with Co = 40 at % deposited at (a) 200 °C and (b) 300 °C.

fluence. Film surfaces in droplet-free areas have been observed at high magnification and films grown on undecapped silicon showed a smooth surface, whereas in films grown on decapped silicon a structure of terrace growth was clearly recognizable (Fig. 1).

The same samples have been observed by TEM. The Co–Ag films of the first group showed a polycrystalline structure with equiaxial grains randomly oriented and a grain size of the order of 15 nm. The corresponding diffraction pattern showed, besides the spots relating to the Si substrate, the diffraction rings typical of a randomly oriented nanocrystalline structure. The angular position of the diffraction rings corresponds to the lattice spacings of the face-centred cubic (fcc) crystal structure of silver without any trace of diffraction effects related to either hexagonal close-packed (hcp) or face-centred cubic (fcc) cobalt. The absence of a Co diffraction pattern, even though X-ray microanalysis confirmed the presence of Co at

the expected concentration, should then be related to the morphology of Co particles or to their presence with highly defective structures. High-resolution images clearly show the presence of an amorphous interlayer 7–10 nm thick between the film and the underlying Si which seems to prevent any form of epitaxy during film growth.

TEM observations made on films grown on decapped silicon showed a structure made of large grains with the silver fcc structure iso-oriented with the Si substrate. In this case too, electron diffraction patterns did not show spots related to the cobalt structure, even if EDS microanalyses showed compositions close to the nominal ones: even for such set of samples, this fact could be explained by assuming a highly defective Co particle structure. TEM images showed a large defect density; in weak-beam dark-field images, where the fine details of the defective structure of the film are better resolved, some globular spots and layered structures lying parallel to (111) lattice planes can be observed.

Chemical composition and profile analyses have been obtained by examining XPS spectra of both the surface and the interior of the films; recording spectra at different etching times, a complete composition profile down to the interface with the silicon substrate has been obtained.

Within a layer of about 1 nm from the surface, a contribution from oxidized species has been observed in the spectra, whereas only pure metallic elements have been detected on scanning throughout the overall film thickness. Within this surface layer, an enrichment of Co has also been observed in some samples, due to the Co diffusion which occurs during thermal treatments. Below the surface layer, a constant atomic percentage of Co and Ag has been observed with values comparable with the nominal ones, thus confirming the EDS analysis. In SEM images of totally etched films, the residual presence of molten metal particulates sticking to the bare substrate has been observed. In such cases, even when the main XPS signal originated from the Si substrate, a weak spurious contribution from metallic elements has been detected, therefore leading to a less clear definition of the interface.

## Magnetic properties investigation

Static magnetization has been measured as a function of temperature in a field  $H_a = 50$  Oe, applied parallel to the film surface, following the zero-field cooling (ZFC) and field cooling (FC) procedures.

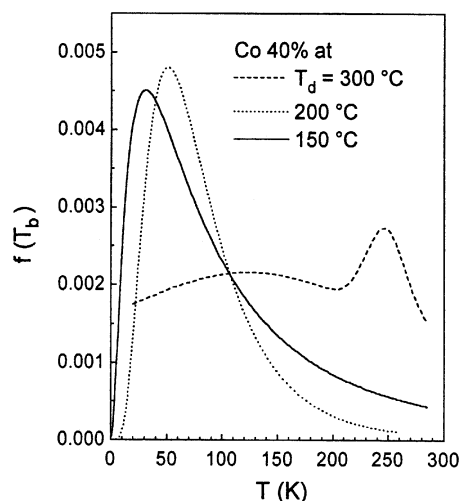


**Figure 3** Distribution functions of blocking temperatures for  $\text{Co}_{40}\text{Ag}_{60}$  deposited at different temperatures.

Since the preparation conditions varied, different behaviours have been observed. For some samples (Fig. 2a) a behaviour typical of superparamagnetic particles, whose moments progressively block with decreasing temperature, has been observed: the ZFC magnetization shows a maximum at  $T = T_{\text{max}}$ , whereas the FC magnetization increases continuously with decreasing temperature. The splitting between the two curves occurs at temperatures higher than  $T_{\text{max}}$ , reflecting the existence of a broad distribution of blocking temperatures ( $T_B$ ). Indeed, the splitting temperature ( $T_{\text{irr}}$ ) corresponds to the highest  $T_B$  and  $T_{\text{max}}$  is related to the average blocking temperature  $\langle T_B \rangle$ , the exact relationship depending on the type of distribution of energy barriers for magnetization reversal.

For other samples (Fig. 2b), no maximum of  $M_{\text{ZFC}}$  has been observed (the magnetization increases continuously with temperature) and the irreversibility appears at  $T > 300$  K. This reflects the existence of a much wider distribution of anisotropy energy barriers, shifted to higher-energy values, i.e. to particles bigger than those belonging to the previous set of samples. Indeed, from the analysis of the temperature variation of the difference between  $M_{\text{FC}}$  and  $M_{\text{ZFC}}$ , the anisotropy energy barrier distribution can in principle be inferred, being  $(M_{\text{FC}} - M_{\text{ZFC}}) \approx \int f(E_B) dE_B$ . Actually, for an assembly of non-interacting particle moments relaxing through a thermally activated mechanism according to an Arrhenius law ( $\tau = \tau_0 \exp E_a/K_b T$ ),  $f(E_B)$  reflects the blocking temperature

distribution  $f(T_B)$ . An analysis of the temperature dependence of the derivative  $d(M_{\text{FC}} - M_{\text{ZFC}})/dT$  has been performed in order to investigate the effect of variation of Co content, deposition and annealing temperature on the energy barrier distribution; such parameters can be varied independently of each other in order to obtain the growth of Co particles of different sizes.

For Co concentrations higher than 30%, at a fixed deposition temperature (i.e. 200 °C), a simple mode distribution has been found, centred between 40 and 50 K. The effect of increasing the Co concentration from 40% to 51% is to produce an increase of the number of particles with the same blocking temperature, the centre of the distribution remaining at almost the same temperature. For concentrations  $\geq 40\%$ , the increase in deposition temperature (up to  $T_{\text{dep}} = 200$  °C) leads to a shift of the distribution maximum to higher temperature (Fig. 3). For  $T_{\text{dep}} \geq 300$  °C, the distribution becomes bimodal with a very broad maximum around 105 K and a narrow one around 245 K, indicating the presence of two distinct sets of particle size. After annealing at 350 °C, the bimodality is removed and the high-temperature maximum becomes predominant.

If the single particle volume anisotropy represents the dominant contribution to the energy barrier, the low-field difference ( $M_{\text{FC}} - M_{\text{ZFC}}$ ) is proportional to:

$$\ln(t_m/\tau_0) \int_{V_c}^{\infty} V f(V) dV$$

where  $V_c$  is the characteristic volume for superparamagnetic relaxation, related to a measuring technique with characteristic time  $t_m$ . Therefore, the derivative  $d(M_{\text{FC}} - M_{\text{ZFC}})/dT$  as a function of temperature yields a direct measure of the particle volume distribution.

For uniaxial anisotropy,  $E_B = K_a V$  and the temperature of the maximum of the distribution (Fig. 3) is related through the Arrhenius law ( $K_b T_B = K_a V \ln(\tau_0/t_m)$ ) to the maximum of the volume distribution. Since TEM results support the presence of a hcp Co defective structure, as a first approximation we used the value of bulk hcp Co ( $K_a = 8 \times 10^6$  erg  $\text{cm}^{-3}$ ) for the anisotropy constant  $K_a$ . Actually, for single domain nanosized particles,  $K_a$  is expected to be higher and then the volume deduced in this way has to be considered as an upper-limit value. This leads to a size distribution centred at a diameter  $\phi \approx 3$  nm for Co concentrations higher than 40%; the increase of the deposition temperature (up to  $T_{\text{dep}} = 200$  °C) leads

to an enlargement of particle size from  $\phi \approx 2.5$  nm to  $\phi \approx 3.5$  nm, whereas for  $T_{\text{dep}} = 300$  °C the observed bimodal distribution corresponds to the presence of two distinct sets of particle sizes ( $\phi \approx 4.5$  nm and  $\phi \approx 6.5$  nm).

## CONCLUSIONS

The microstructural properties of granular Co–Ag thin films have been investigated as a function of Co content, deposition and post-annealing temperature. By the variation of these conditions and the type of substrate pre-treatment, granular as well as crystalline films have been obtained, showing very different structural and morphological properties.

From the analysis of magnetization data, the energy barrier distribution for magnetization reversal was inferred and related to the particle size distribution. Assuming that the dominant contribution to the anisotropy energy comes from the single particle volume anisotropy, it was found that the particle size distribution shifts towards bigger sizes with increasing deposition and annealing temperature. However, for  $T_{\text{dep}} \geq 300$  °C, the size distribution becomes bimodal, centred at  $\phi \approx 4.5$  nm and 6.5 nm. Annealing treatments at  $T_{\text{ann}} = 350$  °C

remove the bimodal character of the distribution, shifting it towards larger particle sizes. Finally, with increasing Co concentration we observed an increment of the average particle size for  $\text{Co} \leq 40\%$ , while, for higher concentrations, the average particle size reaches a constant value (e.g.  $\phi \approx 3.5$  nm for  $T_{\text{dep}} = 200$  °C).

*Acknowledgments* The authors are grateful to Dr G. Righini (ESCALAB, Area della Ricerca di Roma, CNR), Mr P. Filaci and Mr G. Chiozzini for XPS, magnetization and SEM measurements, respectively.

## REFERENCES

1. S. Zhang, *Appl. Phys. Lett.* **61**, 1853 (1992).
2. Y. Huai, M. Chaker, H. Pépin, S. Boily, X. Bian and R. W. Cochrane, *J. Magn. Magn. Mater.* **136**, 204 (1994).
3. T. J. Jackson, S. B. Palmer, H. J. Blythe and A. S. Halim, *J. Magn. Magn. Mater.* **159**, 269 (1996).
4. I. W. Boyd, *The Fourth International Conference on Laser Ablation COLA'97*, July 21–25, Monterey, CA (1997).
5. C. D. Wagner, L. E. Davis, M. V. Zeller, J. A. Taylor, R. M. Raymond and L. M. Gale, *Surf. Interface Anal.* **3**, 211 (1981).
6. E. Sappey, Doctoral Thesis, University of Orsay (Paris), France, 1997.